32ND INTERNATIONAL COSMIC RAY CONFERENCE, BEIJING 2011

Production of secondary cosmic rays in the upper atmosphere

D. MÜLLER[1], P.J. BOYLE[1,3], J.R. HÖRANDEL[2], AND A. OBERMEIER[1,2]
[1] *Enrico Fermi Institute, The University of Chicago, Chicago, USA*
[2] *Department of Astrophysics, Radboud Universiteit, Nijmegen, NL*
[3] *currently at McGill University, Montreal, Canada*

dmuller@uchicago.edu

DOI: 10.7529/ICRC2011/V06/0828

Abstract: The generation of secondary cosmic rays in the residual atmosphere above a high-altitude balloon is a well-known problem that can lead to serious limitations in balloon-borne observations of rare cosmic-ray components. To correct the observations for atmospheric contributions, knowledge of the (partial) interaction cross sections from measurements in the laboratory is required, but often not available with sufficient accuracy. For the TRACER project, this uncertainty affects the determination of the boron-to-carbon (B/C) abundance ratio, which is of critical importance to understand the Galactic propagation of cosmic rays. We therefore also attempt to determine the atmospheric contribution to the data directly by measuring the "growth curve" of atmospheric secondaries, i.e. the measured rate as a function of atmospheric depth. For this we utilize diurnal oscillations in the float altitude of long-duration balloon flights, which amount to several g/cm^2 in column density above the detector. We apply this procedure for the B/C ratio with data obtained in the 2006 balloon flight of TRACER, and we compare the procedure with results obtained when published partial spallation cross sections are used.

Keywords:

1 Introduction

Cosmic-ray measurements on balloon must be corrected to account for particle interactions in the residual atmosphere above the balloon. The atmospheric overburden may be comparable in mass density to the propagation path length in the Galaxy. However, the number of interactions in the atmosphere is smaller than that in the interstellar gas at GeV amu^{-1} energies due to the fact that the interaction mean free path (in g/cm^2) scales roughly with the target mass as $A^{-2/3}$, and that the mass number A of the atmospheric targets is larger than that of the interstellar gas. The attenuation of the particle intensities in the atmosphere is usually calculated using total cross sections for charge-changing interactions in a semi-empirical geometric parameterization [5, 7, 13]. Above a few GeV amu^{-1}, the cross sections are assumed to become independent of energy. In addition to atmospheric losses, one also must take into account the production of particles as daughter products from interactions. This contribution to the measured intensities is especially important for rare secondary cosmic rays, such as the light nuclei Li, Be, and B, as well as anti-protons and positrons. To calculate the intensities of nuclei produced in the atmosphere, one needs to use the partial cross sections for producing a specific secondary element. The most complete compilation of partial cross sections is given by [12]. Naturally, the uncertainties of partial cross sections are larger than those of total cross sections.

An alternative method to account for atmospheric effects that does not depend on explicit knowledge of interaction cross sections, utilizes the determination of "growth curves", i.e. particle intensities as a function of atmospheric depth. Extrapolating measured growth curves to zero depth provides the particle intensity at the top of the atmosphere. However, for a standard balloon flight, the ascent or descent of the payload is too fast for obtaining the growth curve with good statistical accuracy, unless special provisions for a slow descent are made. The situation is different for long-duration balloon flights with zero-pressure balloons: here, the balloon undergoes diurnal fluctuations in altitude, correlated with the sun angle. The amplitude of the fluctuations depends on balloon size and payload weight; a typical maximum height might correspond to about 3 g/cm^2 and minimum height could be around 8 g/cm^2. With flight durations of 30 days or more, this permits continuous measurements of the counting rates as a function of altitude over this range for 30 or more cycles, and may lead to growth curves with rather good statistical accuracy. Note that this approach would not apply to flights with super-pressure balloons.

In the following, we will use the measurement with TRACER of the energy spectrum of boron nuclei and of the

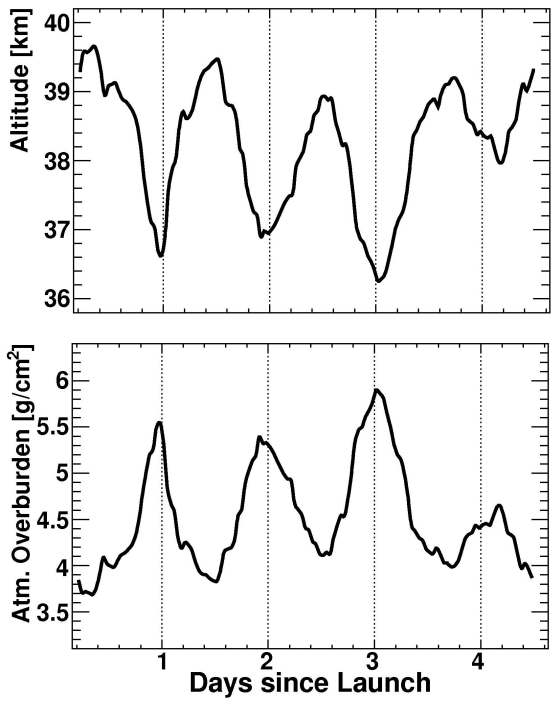

Figure 1: Profiles of altitude and vertical atmospheric overburden as a function of flight time.

abundance of boron relative to the primary parents carbon and oxygen, to illustrate the techniques for the corrections for atmospheric background.

2 Measurement of Growth Curves

The most recent balloon flight of TRACER was conducted in the Northern hemisphere in 2006. The instrument was launched in Kiruna (Sweden), and the flight concluded after about 4.5 days in Northern Canada. More detail about the instrument, flight, data analysis, results and interpretation are given in these proceedings [4, 9], and elsewhere [3, 8]. The profiles of this flight in terms of altitude and atmospheric overburden are shown in Figure 1. One notices pronounced daily variations, with a minimum overburden of 3.7 and a maximum of 5.8 g/cm^2. Unfortunately, the flight had to be terminated after just over 4 cycles for geo-political reasons.

The major goal of this balloon flight was a determination of the relative abundance of the secondary nucleus boron up to energies in the TeV amu^{-1} region. Because of the low particle intensities, one cannot attempt to determine growth curves at the highest energies. However, if we accept energy-independence of the interaction cross sections, we may select the much more plentiful sample of particles with energies just above the level of minimum ionization: here, particles between 3 GeV amu^{-1} and 9 GeV amu^{-1}

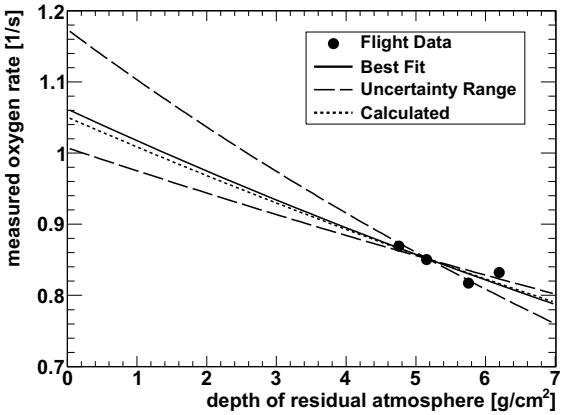

Figure 2: Oxygen rate as a function of atmospheric depth. The best fit to the data (solid line) is shown, as well as its uncertainty range (dashed), and the prediction based on partial cross sections (dotted).

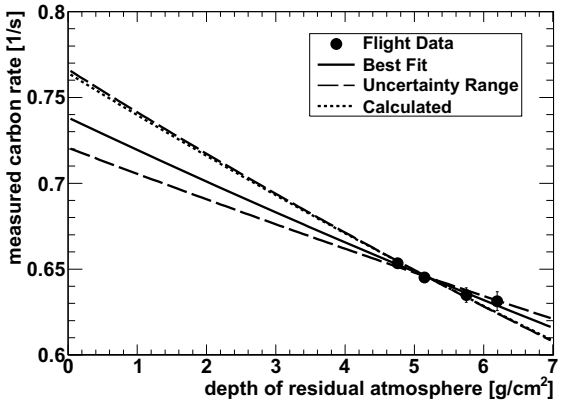

Figure 3: Carbon rate as a function of atmospheric depth. The best fit to the data (solid line) is shown, as well as its uncertainty range (dashed), and the prediction based on partial cross sections (dotted).

are chosen. As examples, the measured count rates for oxygen and carbon nuclei as a function of atmospheric depth are shown in Figures 2 and 3. The same is shown for boron in Figure 4. Exponential fits to the data points are then extrapolated to zero depth.

Inspection of the growth curves reveals that the oxygen and carbon intensities decrease faster with increasing depth than the boron intensity. From the top of the atmosphere to a depth of 5 g/cm^2, the attenuation is about 20% for oxygen and 14% for carbon, whereas boron is attenuated by about 10%. This is to be expected for two reasons: the interaction cross sections for oxygen and carbon are larger than that for boron, and atmospheric production contributes to the intensity of boron, but has only a minor effect on the

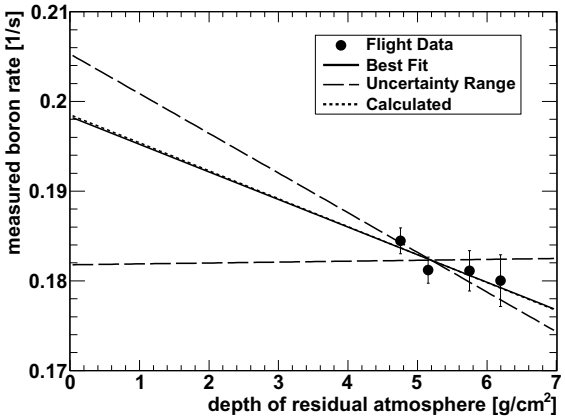

Figure 4: Boron rate as a function of atmospheric depth. The best fit to the data (solid line) determines the production of boron from carbon and oxygen in the atmosphere. The range of the fit uncertainty (dashed) is shown, as well as the prediction (dotted).

more abundant primary elements. The figures also indicate the uncertainty range of the fits. Clearly, the level of accuracy would have been substantially improved with a balloon flight of longer duration.

3 Growth Curves and Interaction Path Lengths

The growth curves for the primary elements oxygen and carbon shown in Figures 2 and 3 are dominantly determined by interaction losses in the atmosphere. Hence, the intensity for primary elements at an atmospheric depth X is (in first order):

$$N_p(X) = N_p(0) \exp\left(-\frac{X}{\Lambda_p}\right) \approx N_p(0)\left(1 - \frac{X}{\Lambda_p}\right), \quad (1)$$

where $\Lambda_p = m/\sigma_p$ is the attenuation path length of the primary element, and m the target nucleus mass. The fit in Figure 2 for oxygen corresponds to $\Lambda_O = 23.4 \pm 7.3$ g/cm^2, in remarkable agreement with an expected value from the geometrical parameterization of 24.6 g/cm^2. A similar comparison for carbon based on the fit of Figure 3 also shows agreement with a fit result of $\Lambda_C = 38.6 \pm 8.4$ g/cm^2 and an expectation value of 30.7 g/cm^2. This expected attenuation path length takes into account the small amount of carbon that is produced by oxygen. Without secondary production, the attenuation path length of carbon would be 27.4 g/cm^2. For oxygen, secondary contribution is insignificant as the heavier elements with $Z > 8$ are rare in cosmic rays.

The intensity profile for boron has two components: Galactic boron, and secondary boron:

$$N_B(X) = N_B(0) \exp\left(-\frac{X}{\Lambda_B}\right) + \sum N_p(0) \frac{X}{\lambda_{p\to B}}. \quad (2)$$

Here, N_p refers to the intensity of a primary nucleus heavier than boron, and $\lambda_{p\to B}$ corresponds to the path length for the production of boron from that primary nucleus. In practice, there are only two significant parent species, carbon and oxygen, both of nearly the same intensity, independent of energy [8, 9]. Equation 2 can then be written as

$$N_B(X) = N_B(0) \exp\left(-\frac{X}{\Lambda_B}\right) + N_C(0) \frac{X}{\lambda_{eff}}, \quad (3)$$

with

$$\lambda_{eff}^{-1} = \lambda_{C\to B}^{-1} + N_O(0)/N_C(0) \cdot \lambda_{O\to B}^{-1}, \quad (4)$$

where $N_C(0)$ and $N_O(0)$ are the carbon and oxygen intensities at $X = 0$, and their ratio is about unity. Thus, one of the components of the growth curve decreases with X, and the other increases linearly. Accepting a value $\Lambda_B = 28.7$ g/cm^2 from the geometrical parametrization of cross sections, the fit in Figure 4 leads to an effective path length of $\lambda_{eff} = 225 \pm 102$ g/cm^2. This value, in spite of the large uncertainty, is in excellent agreement with the effective path length of 227.3 ± 44 g/cm^2 calculated using the cross sections of [12]. The accuracy of the data in Figure 4 is not yet sufficient to provide a stronger constraint on the effective path length than that given by the limits from published values.

4 The B/C Abundance Ratio

We now determine the contribution of atmospheric background to the B/C intensity ratio. To this end, the measured boron intensity is initially treated as if it were of Galactic origin entirely. One would then obtain an apparent intensity $N_B(TOA)$ at the top of the atmosphere (TOA):

$$\begin{aligned} N_B(TOA) &= N_B(X) \exp\left(\frac{X}{\Lambda_B}\right) \\ &= N_B(0) + N_C(0) \cdot \frac{X}{\lambda_{eff}} \exp\left(\frac{X}{\Lambda_B}\right). \end{aligned} \quad (5)$$

For boron, the intensity $N_B(TOA)$ still includes secondary boron nuclei produced from carbon and oxygen in the residual atmosphere. Of course, $N_B(0)$ is the true intensity of boron at $X = 0$. Therefore, the true B/C intensity ratio is

$$\frac{N_B(0)}{N_C(0)} = \frac{N_B(TOA)}{N_C(0)} - \frac{X}{\lambda_{eff}} \exp\left(\frac{X}{\Lambda_B}\right). \quad (6)$$

For any given altitude X, the correction to the apparent B/C ratio at the top of the atmosphere has a constant value, independent of energy. For the TRACER flight, at an average

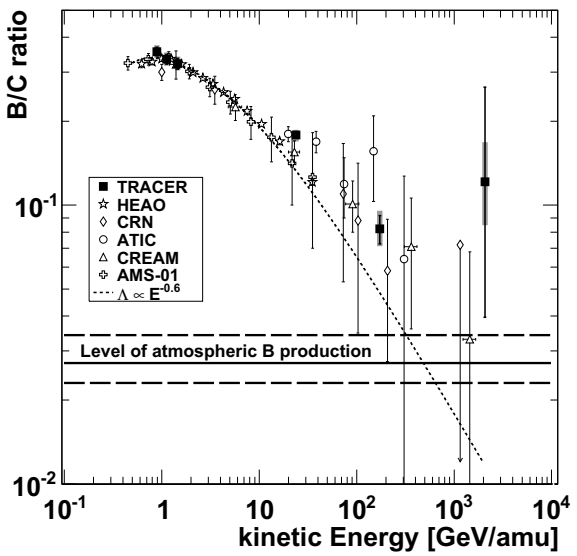

Figure 5: The boron-to-carbon abundance ratio as a function of kinetic energy per nucleon. Error bars are statistical (thin) and systematic (thick). Previous measurements are shown from HEAO [6], CRN [11], ATIC [10], CREAM [2] and AMS-01 [1]. The dotted line indicates an extrapolation for a propagation path length $\propto E^{-0.6}$. The horizontal lines indicate the level of atmospheric boron production and its uncertainty.

altitude $X = 5.2$ g/cm^2, one obtains

$$\frac{X}{\lambda_{eff}} \exp\left(\frac{X}{\Lambda_B}\right) = 0.027^{+0.007}_{-0.004}. \quad (7)$$

The given uncertainties to this number reflect a conservative estimate for calculated path lengths, not for path lengths derived from the growth curves.

The boron to carbon abundance ratio as measured with TRACER, and after subtracting the atmospheric correction (Eq. 7), is shown in Figure 5 as a function of energy. Included for comparison are the results from several other measurements [1, 2, 6, 10, 11]. The magnitude of the atmospheric correction is indicated as a constant line with error limits as in Eq. 7, for $X = 5.2$ g/cm^2. If the B/C ratio continues to decrease towards higher energies, for instance proportional to $E^{-0.6}$ (dotted curve), the B/C ratio would become dominated by background around 1000 GeV amu^{-1}.

5 Discussion and Conclusions

We have used atmospheric growth curves derived from diurnal variations in altitude of a long-duration balloon in order to determine the path lengths for attenuation or secondary generation of cosmic-ray nuclei in the atmosphere. Specifically, we have applied this approach to the measurement of the B/C abundance ratio with the TRACER instrument. The agreement between the empirically determined path lengths and those based on published cross section values is remarkably good. However, the uncertainties in the empirical values are still greater than those corresponding to published numbers. However, there is much room for improvement for the empirical technique: (1) An increase in flight duration by nearly a factor of 10 is possible and would greatly increase the statistical quality and altitude resolution of the growth curves. (2) A more targeted approach than possible for the existing TRACER data can be made to reduce uncertainties due to time-dependent systematic effects, such as dead time fluctuations, gain shifts of detector elements, or time dependence in selection cuts. (3) A dedicated balloon flight would be able to probe a wider range of atmospheric depth and, thus, provide a larger lever arm for the fit, further reducing the uncertainty of the fit results. We presently investigate these options further and will report additional results in due course.

If possible, a higher flight altitude would reduce the magnitude of the atmospheric correction. Of course, the ultimate would be a flight at $X = 0$, but this would require a spacecraft, and is outside the realm of this paper.

Acknowledgements

AO acknowledges support of FOM in the Netherlands ("Stichting voor Fundamenteel Onderzoek der Materie"). This work was supported by NASA through grants NNG 04WC08G, NNG 06WC05G, and NNX 08AC41G.

References

[1] Aguilar M. *et al.* , ApJ, 2010, **724**:329
[2] Ahn H. S. *et al.* , Astro. Ph., 2008, **30**:133
[3] Ave M. *et al.* , NIM A, 2011, in print, DOI: 10.1016/j.nima.2011.05.050
[4] Boyle P. *et al.* , 2011, these proceedings **#707**
[5] Bradt H. L. and Peters B., Phys. Rev., 1950, **77**:54
[6] Engelmann J. J. *et al.* , A&A, 1990, **233**:96
[7] Heckmann H. H. *et al.* , Phys. Rev. C, 1978, **17**:1735
[8] Obermeier A. *et al.* , ApJ, 2011, submitted
[9] Obermeier A. *et al.* , 2011, these proceedings **#675**
[10] Panov A. D. *et al.* , Proc. 30th ICRC, 2007
[11] Swordy S. P. *et al.* , ApJ, 1990, **349**:625
[12] Webber W. R. *et al.* , Phys. Rev. C, 1990, **41**:533
[13] Westfall G. D. *et al.* , Phys. Rev. C, 1979, **19**:1309